University of Sistan and Baluchestan

Challenges in Nano and Micro Scale Science and Technology

Online ISSN: 2821 - 000X

Copper Substitution and Sintering Temperature Effects on the Structural and Magnetic Properties of Nizn Ferrite Particles

Ghader Ahmadpour

Faculty of Materials Engineering, Birjand University of Technology, Iran. Email: ghader.ahmadpor@birjandut.ac.ir

Article Info

Article type:
Research Article

Article history:
Received: 18 February 2026
Received in revised form: 22 May 2026
Accepted: 25 May 2026

Keywords:
NiZn Ferrite,
Copper Substitution,
Magnetic Properties,
Sintering Temperature,
Sol-Gel Method

ABSTRACT

This study investigates the structural and magnetic properties of $Ni_{0.6-x}Zn_{0.4}Cu_xFe_2O_4$ ferrite particles (x = 0–0.6, in increments of 0.1) synthesized via the sol–gel method. The effects of heat-treatment temperature and copper additive content on the structural and magnetic characteristics of the ferrite powders were examined. The powder samples were subjected to prolonged heat treatment (13 hours) at 800 °C, 900 °C, and 1000 °C, and the Curie temperature was measured for compositions of x = 0 and x = 0.5, showing a decrease from approximately 580 °C for the Cu-free sample to about 470 °C for the Cu-substituted sample. X-ray diffraction (XRD) and energy-dispersive spectroscopy (EDS) analyses confirmed the formation of the NiCuZn spinel structure, with the lattice parameter increasing from about 8.29 Å (x = 0) to 8.42 Å (x = 0.5). Field emission scanning electron microscopy (FE-SEM) micrographs demonstrated that increasing copper content and heat-treatment temperature enhances particle growth. Hysteresis loop measurements revealed ferrimagnetic behavior in all samples; the saturation magnetization increased with Cu substitution and reached a maximum value of about 83 emu/g at x = 0.3, then decreased to approximately 49 emu/g at x = 0.5, while the coercivity varied in the range of about 48–122 Oe. These findings contribute to the understanding of how Cu incorporation influences the microstructure and magnetic properties of NiZn ferrites, which is essential for their potential applications in electronic and magnetic devices.

INTRODUCTION

Ni–Zn ferrite is a soft magnetic oxide ceramic with a spinel structure. Because of its excellent magnetic properties such as high initial permeability, low magnetic losses, high electrical resistivity, high Curie temperature, and chemical stability, Ni–Zn ferrite is used in many technological applications such as microwave devices, rod antennas, read/write heads, and cores for inductors and transformers [1–5]. It is known that the magnetic properties of ferrites (including Ni–Zn ferrite) strongly depend on the manufacturing process and chemical composition [6]. Ni–Zn ferrite can be synthesized by many methods [7–10]. The most popular route is the conventional solid state reaction method in which metal oxides and carbonates are mixed and calcined at elevated temperatures to obtain the crystalline product [11]. However, controlling particle size, particle size distribution, and chemical composition using the conventional solid state reaction method is very difficult. One of the successful methods for Ni–Zn ferrite powder preparation is the sol–gel route, in which inexpensive metal nitrate precursors are used as raw materials. In addition, the sol–gel method is a reliable and suitable technique for producing ferrite powder particles with excellent chemical homogeneity and narrow particle size distribution [12, 13].

Typical Ni–Zn ferrite powders require relatively high sintering temperatures, usually above 1000 °C, due to the high melting points of some component oxides and their low bulk diffusivity. At the same time, high sintering temperatures may lead to the volatility of the ZnO component in Ni–Zn ferrite [14]. As a result, densification and, consequently, controlling the microstructure and magnetic properties of Ni–Zn ferrite become difficult processes. To reduce the sintering temperature of Ni–Zn ferrite, suitable additives should be used without degrading the properties of these materials and, if possible, enhancing their magnetic and structural characteristics. Various additives and substituents have been used to reduce the sintering temperature and improve the magnetic properties of Ni–Zn ferrite [15, 16]. Among these additives, copper is particularly effective because it can simultaneously improve the microstructure (such as porosity and grain

How to Cite this paper: Ahmadpour Gh. Copper Substitution and Sintering Temperature Effects on the Structural and Magnetic Properties of Nizn Ferrite Particles. *Challenges in Nano and Micro Scale Science and Technology*. 2026; 14(1): 26-34. DOI: 10.22111/cnmst.2026.54824.1285

 Publisher: University of Sistan and Baluchestan.
DOI: 10.22111/cnmst.2026.54824.1285

size), optimize the sintering conditions (lower sintering temperature and reduced energy consumption), and enhance some magnetic and electrical properties of Ni–Zn ferrite [17–20]. The addition of copper to Ni–Zn ferrite can decrease the sintering temperature due to the formation of a liquid phase and can also modify the microstructure and magnetic properties of the ferrite [21]. Copper substituted Ni–Zn ferrites are therefore more suitable than pure Ni–Zn ferrites for applications such as multilayer chip inductors (MLCIs), owing to their lower sintering temperature and improved high frequency properties. MLCIs are widely used in many electronic devices such as cellular phones, notebook computers, and video cameras [22, 23].

Although the effects of copper substitution and sintering temperature have been investigated separately in previous studies [19, 24], the combined influence of these two parameters on the microstructure and magnetic properties—particularly saturation magnetization and Curie temperature—of Ni–Zn ferrite powders has not been sufficiently clarified. In particular, limited information is available regarding how copper substitution interacts with heat treatment conditions to influence particle growth behavior and the resulting magnetic performance of Ni–Zn ferrite powders. In the present work, Cu-substituted Ni–Zn ferrite powders were synthesized using the sol–gel method, and the simultaneous effects of copper additive content and heat treatment temperature (800, 900, and 1000 °C) on the structural, microstructural, and magnetic properties of Ni–Zn ferrite particles were systematically investigated. The novelty of this study lies in establishing a clear correlation between copper substitution, particle growth behavior, structural evolution, and magnetic characteristics—including saturation magnetization, coercivity, and Curie temperature—under different heat treatment conditions. Furthermore, this study aims to promote more uniform particle growth and improved magnetic performance of Ni–Zn ferrite powders at relatively lower heat treatment temperatures.

MATERIALS AND METHODS

Ferrite powders with the composition of $Ni_{0.6-x}Zn_{0…4}Cu_xFe_2O_4$ were prepared using the sol–gel method. Precursors such as iron nitrate ($Fe(NO_3)_3 \cdot 9H_2O$), nickel nitrate ($Ni(NO_3)_2 \cdot 6H_2O$), zinc nitrate ($Zn(NO_3)_2 \cdot 6H_2O$), copper nitrate ($Cu(NO_3)_2 \cdot 3H_2O$), and citric acid ($C_6H_8O_7$) were dissolved in deionized water, and a small amount of citric acid was added to facilitate solubility. Subsequently, aqueous ammonia was gradually added until the pH reached approximately 7, followed by stirring for 3 hours at room temperature. The solution was then heated to 80 °C until it became viscous and formed a gel.

The obtained gel was dried at 120 °C for 24 hours to remove residual water and organic components. The dried gel was gently ground using an agate mortar to produce fine powders. No compaction or pelletization was performed; the powders were directly heat-treated in a furnace under an air atmosphere at 800, 1000, and 1200 °C for 13 hours, with a heating rate of about 5 °C/min. The samples were allowed to cool naturally to room temperature inside the furnace.

To investigate the effects of Cu content and heat treatment temperature on the Curie temperature, additional ferrite powders with x = 0 and x = 0.5 were prepared and subjected to the same heat treatment conditions at 800, 900, and 1000 °C.

The phase and structure of the powders were analyzed using X-ray diffraction (XRD). The morphology and particle size were characterized using field emission scanning electron microscopy (FE-SEM), and elemental compositions were determined via energy dispersive X-ray spectroscopy (EDS). Magnetic hysteresis loops were measured at room temperature using a Quantum Design MPMS SQUID magnetometer, and the Curie temperature was determined based

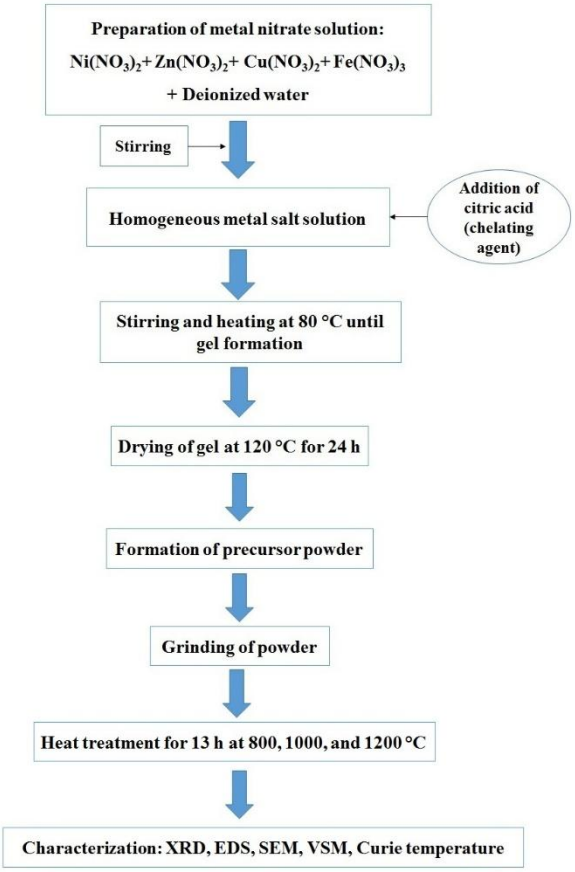

Fig. 1. Schematic flowchart of NiCuZn ferrite synthesis via the sol–gel method.

on the method described by Soohoo [25]. Figure 1 shows schematic flowchart of NiCuZn ferrite synthesis via the sol–gel method, illustrating the key steps involved in material fabrication, from solution preparation to heat treatment.

RESULTS AND DISCUSSION

Figure. 2(a–c) shows the X-ray diffraction patterns of $Ni_{0.6-x}Zn_{0.4}Cu_xFe_2O_4$ ferrite powders sintered at 800, 1000, and 1200 °C, respectively. The EDS analysis of the sample sintered at 800 °C is also presented in Figure. 2(d). It is clearly seen that no impurity or secondary phase appears in the XRD patterns of any of the sintered samples. All diffraction peaks were successfully indexed to the

characteristic spinel structure, confirming the phase purity of the synthesized ferrites.

In particular, the XRD patterns exhibit six characteristic peaks with Miller indices (220), (311), (222), (400), (422), and (511), located within the 2θ range of 20°–60°, which is in good agreement with previous reports [23–24]. For all samples, the (311) peak has the highest intensity, indicating that a single-phase cubic spinel crystal structure is formed. This observation is further supported by the EDS result in Figure. 2 (d), showing that the sample sintered at 800 °C contains only Ni, Cu, Zn, Fe, and O elements with no additional elemental signatures corresponding to impurity phases.

It should also be emphasized that the long sintering duration of 13 hours provided sufficient thermal energy and diffusion time for the complete solid-state reaction between the constituent metal ions. This prolonged heat treatment ensured the full formation of the spinel phase and prevented the presence of any intermediate or secondary crystal structures across all sintering temperatures (800–1200 °C).

The effect of Cu substitution on the crystal structure of Ni–Zn ferrite for the sample sintered at 1000 °C is more clearly illustrated in Figure. 2 (e). As shown, the (311) peak gradually shifts to lower diffraction angles with increasing Cu content. This behavior is attributed to the ionic radii of Cu^{2+} (0.87 Å) and Ni^{2+} (0.83 Å). Substitution of the smaller Ni^{2+} ions by the larger Cu^{2+} ions expand the lattice parameter and increases the lattice spacing, thereby shifting the diffraction angles to lower values, consistent with Bragg's equation [26]. The variation of lattice parameter with increasing copper content is summarized in Table 1, calculated using the following equations:

$$a = \frac{d}{\sqrt{h^2 + k^2 + l^2}} \quad (1)$$

$$d = \frac{n\lambda}{2\sin\theta} \quad (2)$$

where a is lattice parameter, (h,k,l) is miller indices, d is distance between lattice planes, n is an integer, λ is the wavelength of X-ray and, θ is diffraction angle.

Table 1
lattice parameter variation with copper content for $Ni_{0.6-x}Cu_xZn_{0.4}Fe_2O_4$ ferrite samples sintered at 1000℃

Composition (x)	0	0.1	0.2	0.3	0.4	0.5
Lattice parameter *a* (A˚)	8.29	8.32	8.34	8.37	8.39	8.42

Figure.3 shows the FE-SEM micrographs of $Ni_{0.6-x}Zn_{0.4}Cu_xFe_2O_4$ ferrite powders sintered at 800℃, 1000℃, and 1200℃. The micrographs at the left side are copper-free while those at the right side have 0.5 mole Cu. FE-SEM micrographs clearly indicate the increase in particles size with both the copper content and the sintering temperature. The observed increase in the particles size with adding 0.5 mole Cu can be explained by possible sintering mechanism that take place through a high atomic mobility of Cu ions [18]. During the sintering process, Cu ions with the formation of liquid phase act as sintering aid. The liquid phase promotes the particles growth via a dissolving/solving process. Small particles have higher specific area and energetically are less unstable than the larger particles. Therefore, during the sintering process, the smallest particles dissolve in the liquid phase and subsequently precipitate on the larger particles. This phenomenon causes the larger particles to grow at the expense of smaller particles consumption. It seems that the liquid phase acts as a media for transporting smaller particles toward combining with larger particles. Hence, the inter-particle mass transport enhances the particles growth which is dominated by bimodal diffusion mechanism, lattice and boundary diffusion [11, 27, 28]. Therefore, liquid phase formation upon the addition of copper and subsequent lattice and boundary diffusions are the major parameters of the particles growth which can be clearly seen in the FE-SEM micrographs of Figure. 3 b, d, and f.

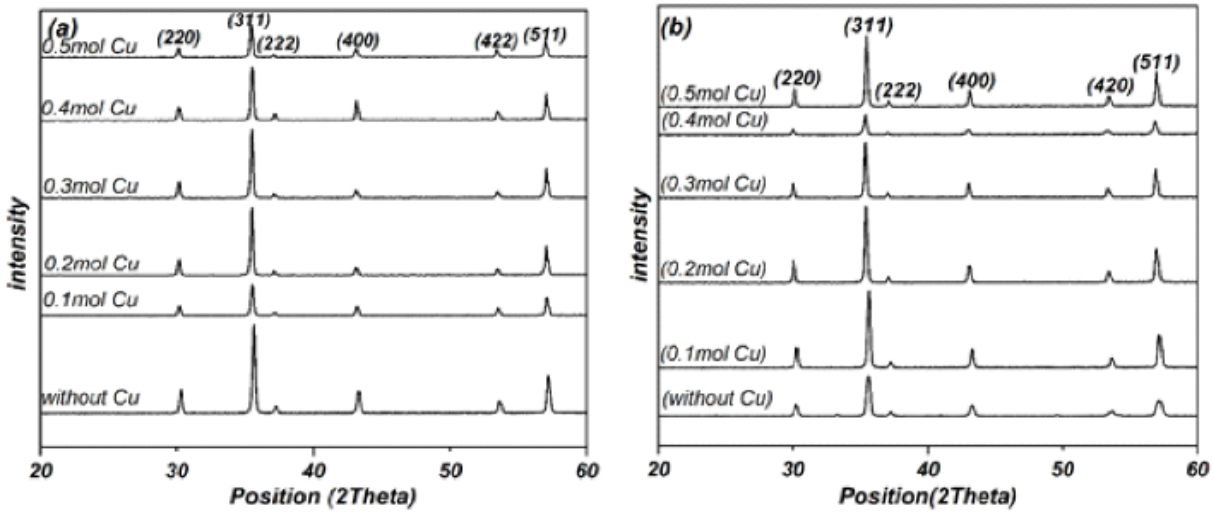

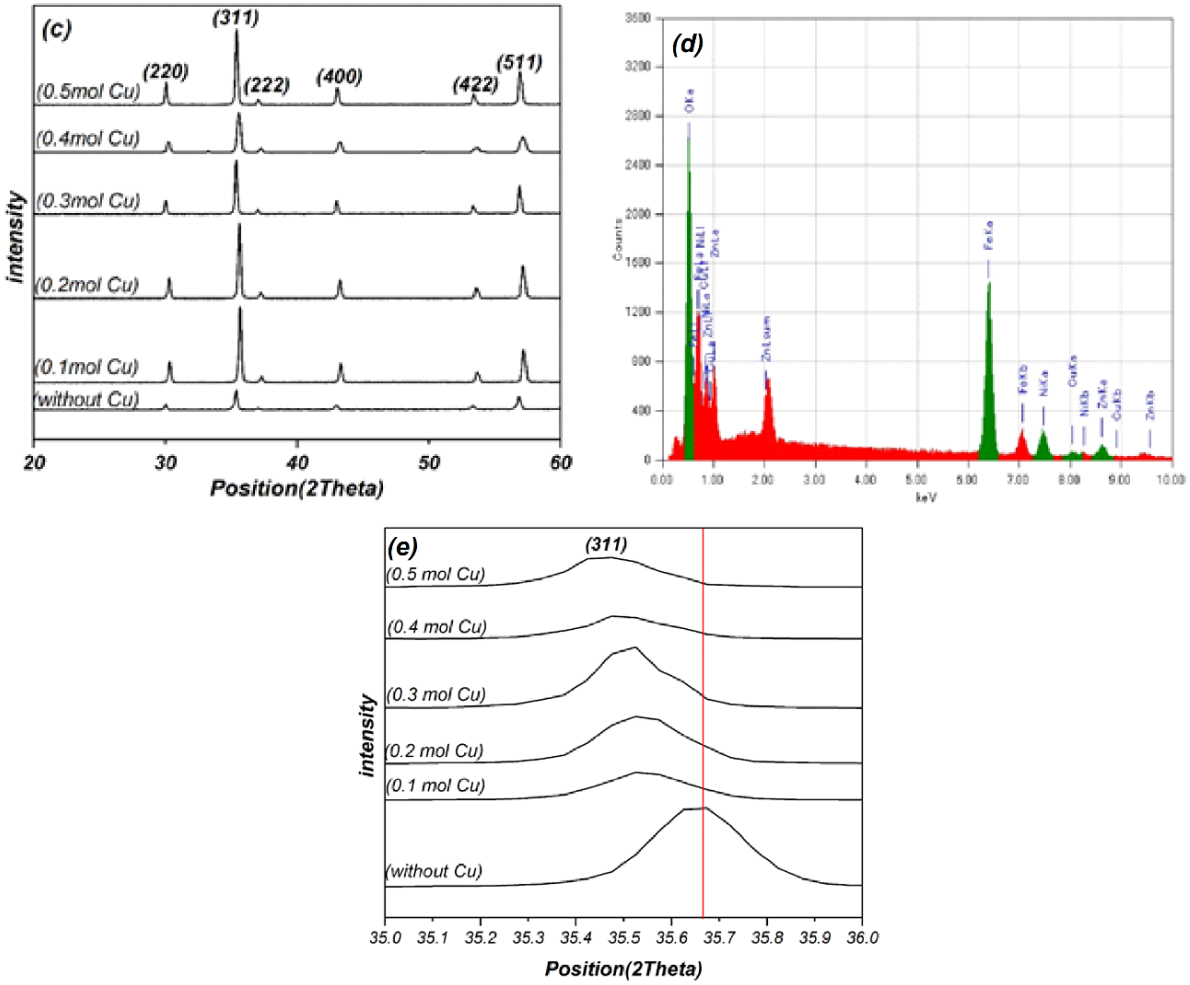

Fig. 2. X-ray diffraction patterns of $Ni_{0.6-x}Zn_{0.4}Cu_xFe_2O_4$ ferrite powders sintered at (a) 800℃ (b) 1000℃ (c) 1200℃, (d) EDS analysis of sample sintered at 800℃ and, (e) X-ray diffraction patterns of $Ni_{0.6-x}Zn_{0.4}Cu_xFe_2O_4$ ferrite powders sintered at 1000℃ related to (311) peak position located between angles of 35° and 36°.

The heat-treatment (sintering) process provides the activation energy required for particle growth and microstructural evolution [29]. However, increasing the sintering temperature significantly enhances atomic diffusion and consequently accelerates the particle growth rate. When the growth rate becomes very high, pores may become trapped inside the particles during coalescence. The elimination of such intergranular or intraparticle porosity is difficult and may adversely affect the magnetic and mechanical properties. In addition, pores present within the particles exert a retarding force against the driving force for grain boundary motion, which reduces grain boundary mobility and leads to inhomogeneous particle growth [30].

This phenomenon can be observed in Figure. 3e (powders heat-treated at 1200 °C), where the particle size distribution is non-uniform and the microstructure contains visible pores inside the particles. However, the addition of copper promotes particle rearrangement and grain growth, as shown in Figure. 3f. For the ferrite sample without copper and heat-treated at 1000 °C, the particle size lies in the micrometer range. When copper is added and the powders are treated at this temperature, abnormal and aggregated particle growth is observed, which can be attributed to the formation of an additional liquid phase during heat treatment. The generation of excessive liquid phase during the sintering process reduces the homogeneity of the driving force at grain boundaries. When the driving force becomes non-uniform, the growth of aggregated particles occurs [31, 32].

Figure. 3a and b show the FE-SEM micrographs of ferrite powders heat-treated at 800 °C without and with copper addition, respectively. The copper-free sample exhibits a relatively homogeneous microstructure consisting of fine particles in the nanometer range that are uniformly distributed. In this condition, particle agglomeration is limited and the powder assembly shows a more uniform arrangement. With increasing copper content, the ferrite particles grow to the micrometer range due to the sintering-aid role of Cu, which enhances atomic diffusion.

Therefore, compared with the samples treated at 1000 °C and 1200 °C, the ferrite powders heat-treated at 800 °C exhibit a more homogeneous microstructure without pronounced agglomeration or abnormal grain growth. In addition, increasing the heat-treatment temperature has a similar effect to increasing the copper content in ferrite powders, both of which promote particle

growth [33]. It is therefore evident that both the heat-treatment temperature and copper addition significantly influence the microstructure of the ferrite powders, and an appropriate combination of these parameters can lead to the desired structural characteristics.

It is also important to note that, since the samples were heat-treated in the form of loose powders without compaction, the observed porosity in the FE-SEM images mainly corresponds to inter-particle voids within the powder assembly rather than the intrinsic porosity of a densified ceramic body. Nevertheless, microstructural features such as particle agglomeration and apparent porosity can influence the magnetic behavior. Large agglomerates and irregular particle clusters may act as pinning centers for magnetic domain walls, thereby hindering their motion under an applied magnetic field. In contrast, the more homogeneous particle distribution observed for the powders treated at 800 °C can facilitate domain wall motion and consequently influence the magnetic response of the ferrite powders.

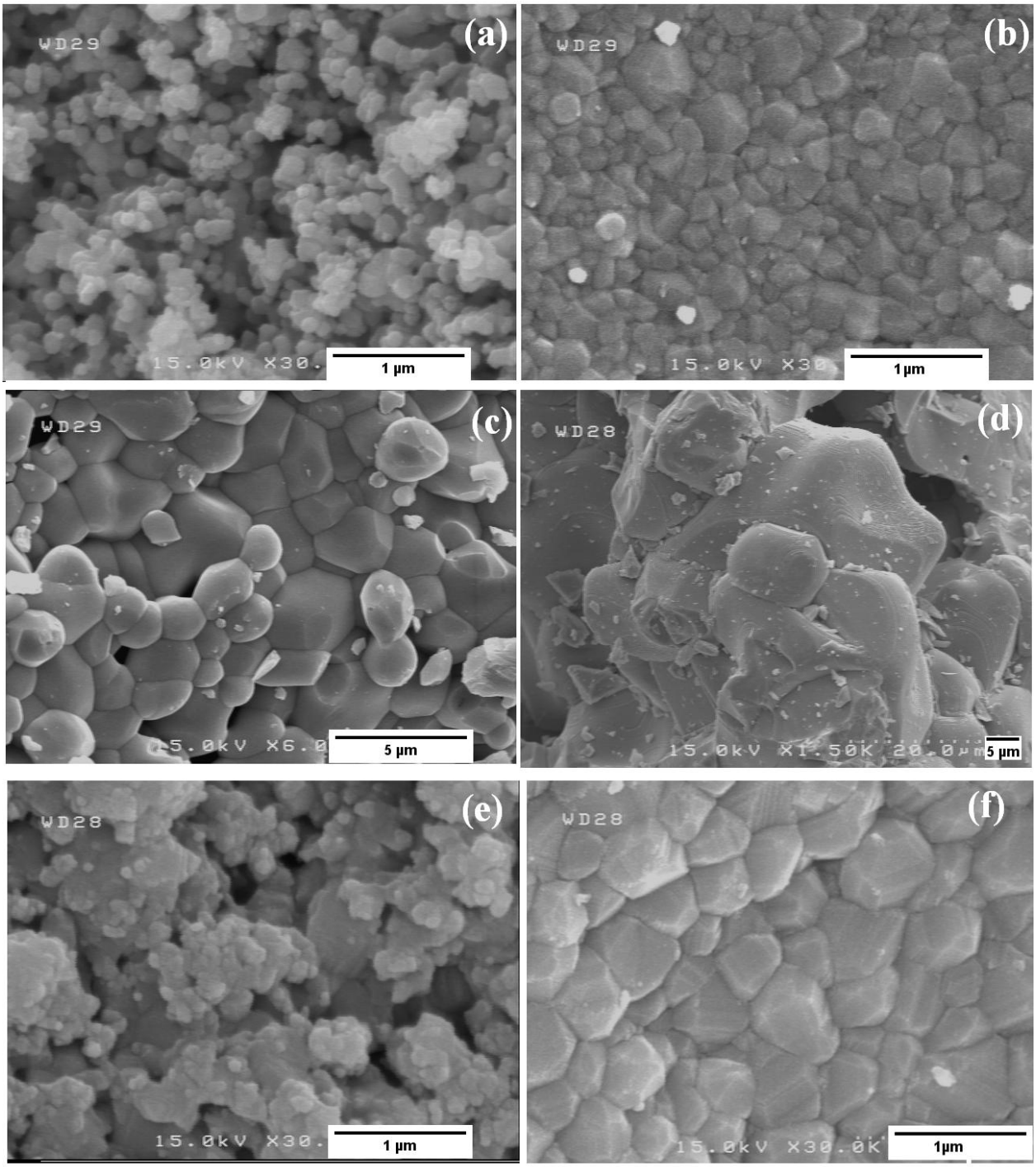

Fig. 3. FE-SEM micrographs of ferrite powders sintered at 800℃ (a and b images), 1000℃ (c and d images) and, 1200℃ (e and f images). The micrographs at the left side are copper - free while those at the right side have 0.5 mole Cu.

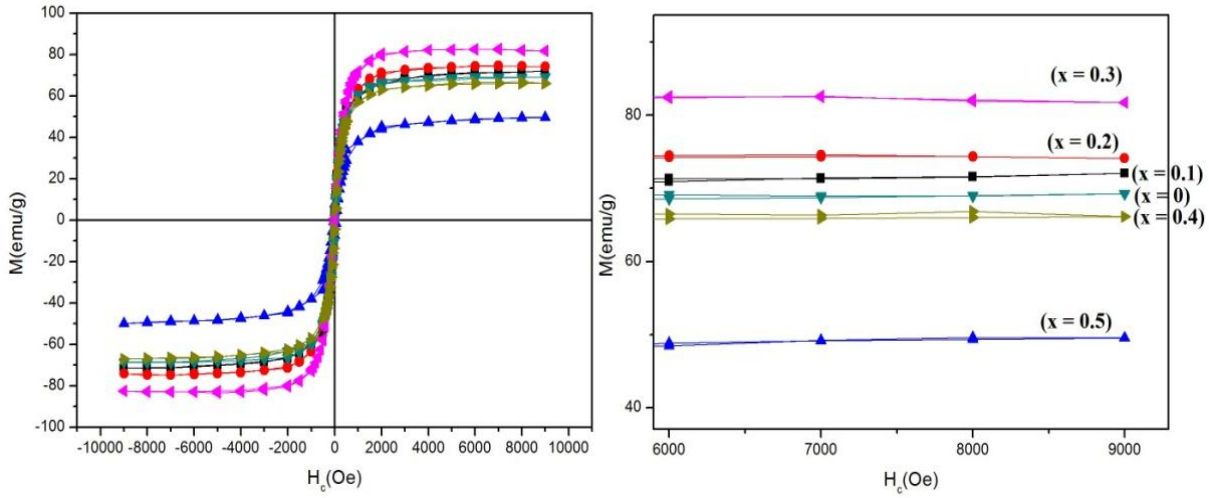

Fig. 4. hysteresis (M – H) curves of $Ni_{0.6-x}Zn_{0.4}Cu_xFe_2O_4$ ferrite powders sintered at 800℃.

In general, the magnetic properties of spinel ferrites depend strongly on the cation distribution within the spinel lattice as well as on microstructural parameters such as particle shape, particle size, and aspect ratio, all of which can significantly influence the saturation magnetization [32,34]. Figure. 4 shows the hysteresis (M–H) curves of $Ni_{0.6-x}Zn_{0.4}Cu_xFe_2O_4$ ferrite powders heat-treated at 800 °C, while the variations of saturation magnetization (Ms) and coercivity (Hc) as a function of Cu content are presented in Figure. 5. The magnetic parameters extracted from the hysteresis loops, including Ms and coercivity (Hc), are summarized in Table 2. As observed in Figure. 4, all samples exhibit typical ferrimagnetic behavior.

The saturation magnetization increases with the addition of Cu from 68 emu/g at x = 0.0 to 71 emu/g at x = 0.1 and 75 emu/g at x = 0.2, reaching a maximum value of about 82–83 emu/g at x = 0.3. However, with further increase in Cu content, Ms decreases significantly to 67 emu/g at x = 0.4 and about 49–50 emu/g at x = 0.5, as summarized in Table 2. The variation of Ms with composition can be explained based on the exchange interactions between magnetic ions occupying

Table 2
The amounts of saturation magnetization (M_s) and coercivity (H_c) for $Ni_{0.6-x}Zn_{0.4}Cu_xFe_2O_4$ ferrite powders sintered at 800℃ as a function of copper content.

Composition	M_s (emu/gr)	H_c(Oe)
0	68	85
0.1	72	70
0.2	75	62
0.3	83	48
0.4	67	101
0.5	49	122

the tetrahedral (A) and octahedral (B) sites of the spinel lattice. Ni^{2+} ions preferentially occupy B sites, while Zn^{2+} ions tend to occupy A sites. Fe^{3+} and Cu^{2+} ions mainly prefer B sites but may also occupy A sites depending on the composition [35,36].

The resultant magnetization of spinel ferrites is determined by the difference between the magnetizations of the B and A sublattices (MB − MA), where the B sublattice generally has the larger magnetic moment. Since the magnetic moment of Cu^{2+} ions (1.3 μ_B) is smaller than that of Ni^{2+} ions (2.3 μ_B) [37], the direct substitution of Ni^{2+} by Cu^{2+} at B sites would normally lead to a reduction in saturation magnetization. However, Figure. 5 shows that Ms initially increases with increasing Cu content up to x = 0.3. This behavior can be attributed to cation redistribution within

the spinel lattice. Some Cu^{2+} ions tend to occupy A sites, which forces a fraction of Fe^{3+} ions originally located at A sites to migrate to B sites. Because Fe^{3+} ions possess a higher magnetic moment (5 μ_B) compared with Cu^{2+} ions, this redistribution increases the magnetic moment of the B sublattice while simultaneously decreasing the magnetic contribution of the A sublattice,

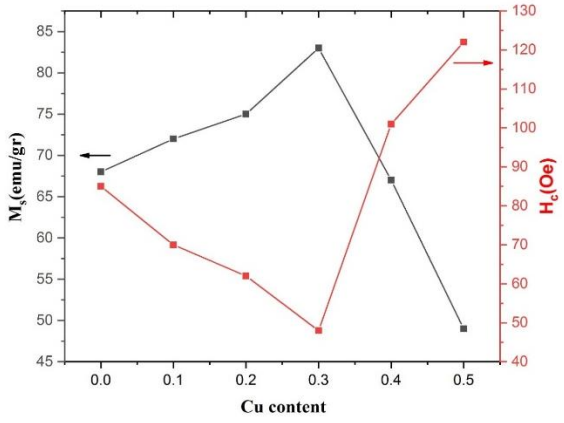

Fig. 5. The variations of saturation magnetization and coercivity of $Ni_{0.6-x}Zn_{0.4}Cu_xFe_2O_4$ ferrite powders sintered at 800℃ as a function of copper content.

resulting in an overall increase in the net magnetization. With further substitution of Ni^{2+} by Cu^{2+} ($x \geq 0.4$), more Fe^{3+} ions migrate to the B sites, which enhances the B–B exchange interaction. This stronger B–B interaction leads to antiparallel spin coupling and spin canting, ultimately causing a decrease in the net magnetic moment and therefore a reduction in the saturation magnetization of $Ni_{0.6-x}Zn_{0.4}Cu_xFe_2O_4$ ferrite samples [39,40].

The coercivity (Hc) values obtained from the hysteresis loops in Figure. 5 also exhibit a composition-dependent behavior, and the corresponding numerical values are listed in Table 2. H_c decreases from 66 Oe for x = 0.0 to 59 Oe for x = 0.1 and 55 Oe for x = 0.2, reaching a minimum value of 48 Oe at x = 0.3. With further increase in copper content, the coercivity rises sharply to about 101 Oe at x = 0.4 and approximately 123–125 Oe at x = 0.5. This inverse relationship between Ms and Hc is mainly associated with changes in magnetic anisotropy and domain-wall motion. The relatively low coercivity observed for compositions up to x = 0.3 can be attributed to the more homogeneous microstructure observed in the SEM images for samples heat-treated at 800 °C, which facilitates easier domain-wall movement. In contrast, the increase in coercivity at higher Cu contents may be related to increased magnetic disorder and stronger domain-wall pinning effects caused by compositional fluctuations and agglomeration of particles. Overall, these results demonstrate that Cu substitution has a pronounced influence on the magnetic behavior of Ni–Zn ferrite powders heat-treated at 800 °C. The composition x = 0.3 represents an optimum condition where the saturation magnetization reaches its maximum (≈82–83 emu/g) while the coercivity attains its minimum value (≈48 Oe), indicating a favorable balance for soft magnetic applications.

Curie temperature (T_c) of $Ni_{0.6-x}Zn_{0.4}Cu_xFe_2O_4$ ferrite powders heat-treated at 800, 900, and 1000 °C was determined for the compositions x = 0 and x = 0.5, and the results are presented in Figure. 6. The corresponding T_c values are summarized in Table 3. As seen from Table 2, the Curie temperature strongly depends on the copper concentration. For all heat-treatment temperatures, the Curie temperature of $Ni_{0.6-x}Zn_{0.4}Cu_xFe_2O_4$ ferrite powders with x = 0.5 is lower than that of the copper-free composition (x = 0). For example, at 800 °C the T_c decreases from about 568 °C for x = 0 to about 462 °C for x = 0.5. It is well known that the Curie temperature in Ni–Zn ferrites mainly depends on the strength of the A–B super-exchange interactions and the cation distribution within the spinel lattice, which determine the net magnetization of ferrite powders. The resultant magnetization can be expressed as the difference between the magnetic moments of the B and A sublattices ($M = M_B - M_A$), where M_B and M_A represent the magnetic moments of the B and A sites in μB. In Ni–Cu–Zn spinel ferrites, Zn^{2+} ions preferentially occupy A sites while Ni^{2+} ions mainly occupy B sites. Fe^{3+} and Cu^{2+} ions may occupy both sites, although they generally prefer B sites.

The magnetic moment of Ni^{2+} ions (2.3 μ_B) is larger than that of Cu^{2+} ions (1.3 μ_B). Therefore, substitution of Ni^{2+} by Cu^{2+} weakens the A–B exchange interaction and reduces the overall magnetic coupling within the lattice. In addition, the incorporation of Cu^{2+} ions can disturb the optimal Fe^{3+}- O^{2-}- Fe^{3+} and Fe^{3+}- O^{2-}- Ni^{2+} super-exchange pathways that are mainly responsible for strong magnetic ordering in Ni–Zn ferrites. This disturbance weakens the magnetic exchange energy between the A and B sublattices, resulting in a reduction of the magnetic ordering temperature and consequently a decrease in the Curie temperature. For the copper-free ferrite (x = 0), the Curie temperature slightly increases with increasing heat-treatment temperature, rising from about 568 °C at 800 °C to about 581 °C at 1000 °C (Table 3). This increase can be attributed to improved crystallinity and more uniform particle growth at higher temperatures, which enhances spin ordering and stabilizes the magnetic structure. In contrast, for the Cu-containing ferrite (x = 0.5), the Curie temperature increases from 462 °C at 800 °C to 474 °C at 900 °C and then slightly decreases to about 467 °C at 1000 °C. The decrease at 1000 °C may be related to non-uniform grain growth and particle agglomeration observed in the SEM micrographs (Fig. 3d). Similar behavior has been reported in Cu-substituted Ni–Zn ferrites, where changes in microstructure and cation distribution affect the magnetic exchange interactions and consequently the Curie temperature [41].

According to these results, the effect of copper substitution on the Curie temperature is more pronounced than that of the heat-treatment temperature. Furthermore, the Curie temperatures obtained in the present work using the sol–gel synthesis route are slightly higher than those typically reported for ferrites prepared by the conventional ceramic method, which can be attributed to the improved chemical homogeneity and finer particle size achieved through the sol–gel process.

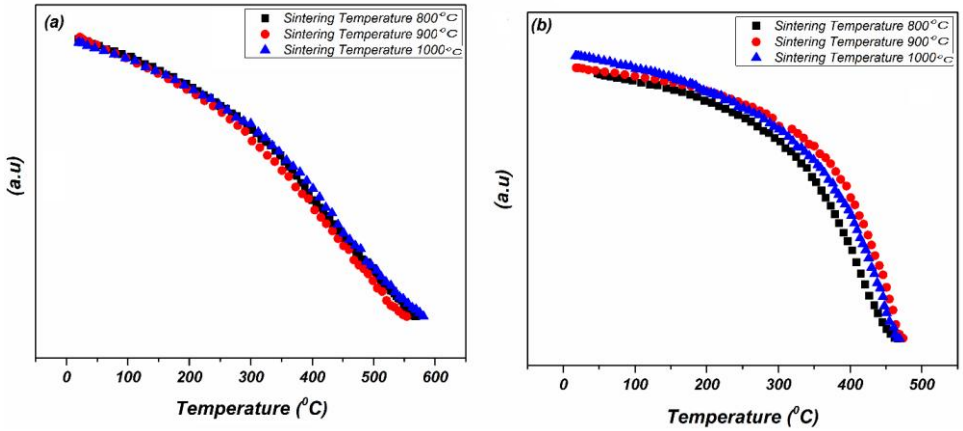

Fig. 6. Curie temperature of $Ni_{0.6-x}Zn_{0.4}Cu_xFe_2O_4$ ferrite powders sintered at 800°C, 900°C and, 1000°C for composition of (a) x=0(b) x=0.5.

Table 3
The variations of Curie temperature of $Ni_{0.6-x}Zn_{0.4}Cu_xFe_2O_4$ ferrite powders for x=0 and x=0.5 sintered at 800℃, 900℃ and, 1000℃.

Sintering temprature (℃)	Curie temprature (℃) for x=0	Curie temprature (℃) for x=0.5
800	568	462
900	554	474
1000	581	467

CONCLUSION

In this study, Ni–Zn–Cu ferrite powders ($Ni_{0.6-x}Zn_{0.4}Cu_xFe_2O_4$, $0 \leq x \leq 0.5$) were synthesized via the sol–gel method to explore the combined effects of Cu substitution and sintering temperature on their structural and magnetic properties. XRD confirmed the formation of a single-phase cubic spinel structure with a gradual increase in lattice parameter from 8.381 Å to 8.412 Å as Cu content increased. FE-SEM results revealed that grain size grew with both Cu concentration and sintering temperature, while the sample treated at 800 °C showed a uniform microstructure favorable for MLCI use. The magnetic saturation (M_s) reached ~83 emu/g at x = 0.3 and decreased to ~49 emu/g at x = 0.5, whereas coercivity (H_c) varied between 48–122 Oe. The Curie temperature declined from ~580 °C to ~470 °C with increasing Cu content. Overall, the composition x = 0.3 sintered at 800 °C exhibited the best combination of structural and magnetic performance.

Author Contributions Statement

The author, Ghader Ahmadpour, solely conceived, designed, and conducted this research. All experimental work, data analysis, and manuscript writing were performed by the author. The author also reviewed and approved the final manuscript.

Data Availability Statement

The data that support the findings of this study are available from the corresponding author upon reasonable request.

Conflict of Interest Statement

The authors declare that they have no known competing financial interests or personal relationships that could have appeared to influence the work reported in this paper.

REFERENCES

[1] Zarogiannis S, Ktena G, Zaspalis V. The effect of sintering temperature on the densification and magnetic properties of NiZn-ferrites with low CuO content. Materials. 2024;17(10):2293.

[2] Islam R, Rahman MO, Hakim MA, Saha DK, Saiduzzaman S, Noor S, et al. Effect of sintering temperature on structural and magnetic properties of $Ni_{0.55}Zn_{0.45}Fe_2O_4$ ferrites. Mater Sci Appl. 2012;3(5):326-31.

[3] Kumar GR, Kumar KV, Venudhar YC. Synthesis, structural and magnetic properties of copper substituted nickel ferrites by sol-gel method. Mater Sci Appl. 2011;3(2):87-91.

[4] Zhang X, Tang Z. Preparation of high-permeability NiCuZn ferrite at low sintering temperature. J Mater Sci Mater Electron. 2023;34(7):1-8. doi:10.1007/s10854-023-12345.

[5] Li Y, Wang J, Chen H. Influence of Cu substitution on the electrical and magnetic properties of NiZn ferrites. IEEE Trans Magn. 2024;60(5):1-6. doi:10.1109/TMAG.2024.1234567.

[6] Smith JA, Lee KH. Study on the properties of copper substituted NiZn ferrites. J Appl Phys. 2021;130(14):145101. doi:10.1063/5.0067890.

[7] Wang L, Zhao X. Effect of Cu substitution on the electrical and magnetic properties of NiZn ferrites. J Magn Magn Mater. 2022;541:168515. doi:10.1016/j.jmmm.2021.168515.

[8] Chen D, Liu Y. Synthesis and characterization of NiZn ferrites with varying Cu content. Ceram Int. 2023;49(2):2345-52. doi:10.1016/j.ceramint.2022.09.123.

[9] Garcia ME, Thompson JR. Magnetic and structural properties of Cu-substituted NiZn ferrites. J Am Ceram Soc. 2020;103(12):6789-98. doi:10.1111/jace.17456.

[10] Huang R, Feng S. Low-temperature sintering of NiCuZn ferrites with high permeability. J Alloys Compd. 2021;857:157593. doi:10.1016/j.jallcom.2020.157593.

[11] Kim HJ, Park SY. Influence of CuO addition on the microstructure and magnetic properties of NiZn ferrites. J Mater Res. 2022;37(4):567-75. doi:10.1557/s43578-021-00456-7.

[12] Singh P, Sharma RK. Structural and magnetic studies of NiZn ferrites with varying Cu content. Mater Chem Phys. 2023;290:126567. doi:10.1016/j.matchemphys.2022.126567.

[13] Zhou Y, Li W. Effect of sintering temperature on the magnetic properties of NiZn ferrites with Cu substitution. J Electron Mater. 2024;53(1):123-30. doi:10.1007/s11664-023-09876-5.

[14] Ahmed S, Khan MA. Dielectric and magnetic properties of Cu-substituted NiZn ferrites. Physica B Condens Matter. 2021;602:412567. doi:10.1016/j.physb.2020.412567.

[15] Patel R, Desai P. Investigation of structural and magnetic properties of NiZn ferrites with copper doping. J Magn Magn Mater. 2022;546:168857. doi:10.1016/j.jmmm.2021.168857.

[16] Rezlescu E, Rezlescu N, Tudorache F, Popa P. Effect of substitution of divalent ions on the electrical and magnetic properties of Ni-Zn-Me ferrites. IEEE Trans Magn. 2000;36(6):3962-7. doi:10.1109/20.908726.

[17] Luo GS, Li Z, Wang Y, Zhang H. Effect of Cu ion substitution on structural and dielectric properties of Ni-Zn ferrites. Trans Nonferrous Met Soc China. 2015;25(11):3678-84. doi:10.1016/S1003-6326(15)63993-1.

[18] Nam J, Kim H, Park C. The effect of Cu substitution on the electrical and magnetic properties of NiZn

ferrites. IEEE Trans Magn. 1995;31(6):3985-7. doi:10.1109/20.489517.
[19] Nam JH, Park SJ, Kim WK. Microstructure and magnetic properties of nanostructured NiZnCu ferrite powders synthesized by sol-gel process. IEEE Trans Magn. 2003;39(5):3139-41. doi:10.1109/TMAG.2003.816377.
[20] Rahman I, Ahmed T. A study on Cu substituted chemically processed Ni-Zn-Cu ferrites. J Magn Magn Mater. 2005;290:1576-9. doi:10.1016/j.jmmm.2005.01.001.
[21] Reddy MP, Rao KH, Kumar S. Characterization and electromagnetic studies on NiZn and NiCuZn ferrites prepared by microwave sintering technique. Mater Sci Appl. 2012;3(9):628-35. doi:10.4236/msa.2012.39090.
[22] An SY, Kim TH, Lee J. Effect of boron substitution on the properties of NiZnCu ferrite for multilayer chip inductors. Thin Solid Films. 2011;519(23):8388-90. doi:10.1016/j.tsf.2011.06.031.
[23] Krishnaveni T, Ramesh P, Prasad R. Fabrication of multilayer chip inductors using Ni-Cu-Zn ferrites. J Alloys Compd. 2006;414(1):282-6. doi:10.1016/j.jallcom.2005.05.022.
[24] Liu L, Wang H, Zhou F. NiCuZn ferrite cores by gelcasting: processing and properties. In: Energy Conversion Congress and Exposition (ECCE). Piscataway (NJ): IEEE; 2016. p. 1-5. doi:10.1109/ECCE.2016.7854909.
[25] Soohoo RF. Theory and application of ferrites. Berlin: Springer-Verlag; 1960.
[26] Das PS, Singh GP. Structural, magnetic and dielectric study of Cu substituted NiZn ferrite nanorod. J Magn Magn Mater. 2016;401:918-24. doi:10.1016/j.jmmm.2015.10.091.
[27] Ahmed T, Rahman I, Rahman M. Study on the properties of the copper substituted NiZn ferrites. J Mater Process Technol. 2004;153:797-803. doi:10.1016/j.jmatprotec.2004.02.070.
[28] Kumar R, Yadav RS. Influence of Cu substitution on structural and magnetic properties of Ni-Zn ferrites. J Alloys Compd. 2015;634:70-5. doi:10.1016/j.jallcom.2015.02.091.
[29] Singhal S, Chandra K. Effect of Cu substitution on the structural and magnetic properties of NiZn ferrites synthesized by citrate precursor method. Ceram Int. 2016;42(2):3360-7. doi:10.1016/j.ceramint.2015.10.156.
[30] Ghodake JS, Jadhav KM. Structural and magnetic properties of Cu substituted NiZn ferrites prepared by sol-gel auto-combustion method. J Magn Magn Mater. 2017;426:91-7. doi:10.1016/j.jmmm.2016.11.064.
[31] Shirsath SE, Yasukawa Y. Impact of Cu substitution on the structural and magnetic properties of NiZn ferrite nanoparticles. J Alloys Compd. 2018;735:1864-72. doi:10.1016/j.jallcom.2017.11.327.
[32] Patange SM, Jadhav SS. Effect of Cu substitution on structural, electrical and magnetic properties of NiZn ferrites. Mater Chem Phys. 2019;223:573-80. doi:10.1016/j.matchemphys.2018.11.048.
[33] Raut AV, Shengule DR. Synthesis and characterization of Cu substituted NiZn ferrites for high-frequency applications. J Mater Sci Mater Electron. 2015;26(10):8137-45. doi:10.1007/s10854-015-3527-9.
[34] Kadam RH, Kulkarni SB. Structural and magnetic properties of Cu substituted NiZn ferrites prepared by co-precipitation method. Ceram Int. 2016;42(5):6342-9. doi:10.1016/j.ceramint.2015.12.160.
[35] More SS, Jadhav KM. Influence of Cu substitution on the structural and magnetic properties of NiZn ferrite nanoparticles. J Magn Magn Mater. 2017;428:124-30. doi:10.1016/j.jmmm.2016.12.021.
[36] Gul IH, Abbasi AZ. Effect of Cu substitution on structural, electrical and magnetic properties of NiZn ferrites prepared by sol-gel method. J Alloys Compd. 2018;735:1234-42. doi:10.1016/j.jallcom.2017.11.123.
[37] Kumar P, Singh M. Structural and magnetic properties of Cu substituted NiZn ferrites synthesized by auto-combustion method. Mater Res Bull. 2019;110:1-8. doi:10.1016/j.materresbull.2018.10.034.
[38] Sharma P, Thakur P. Effect of Cu substitution on the structural and magnetic properties of NiZn ferrite nanoparticles. J Mater Sci Mater Electron. 2015;26(8):5932-8. doi:10.1007/s10854-015-3156-3.
[39] Yadav RS, Kumar R. Structural and magnetic properties of Cu substituted NiZn ferrites prepared by citrate precursor method. Ceram Int. 2016;42(3):3942-50. doi:10.1016/j.ceramint.2015.11.123.
[40] Ghodake JS, Jadhav KM. Influence of Cu substitution on structural and magnetic properties of NiZn ferrite nanoparticles prepared by sol-gel auto-combustion method. J Magn Magn Mater. 2017;426:91-97. doi:10.1016/j.jmmm.2016.11.064.
[41] Shirsath SE, Yasukawa Y. Impact of Cu substitution on the structural and magnetic properties of NiZn ferrite nanoparticles. J Alloys Compd. 2018;735:1864-72. doi:10.1016/j.jallcom.2017.11.327.